International Conference on Space Optics—ICSO 2006

Noordwijk, Netherlands

27–30 June 2006

Edited by Errico Armandillo, Josiane Costeraste, and Nikos Karafolas

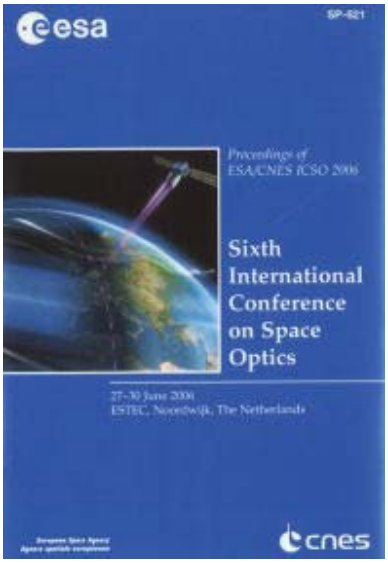

A comparative analysis at engineering level of dispersive and Fourier transform spectrometers for MTG sounding applications

Mathieu Quatrevalet, Donny Aminou, Jean-Loup Bézy

esa icso proceedings cnes

International Conference on Space Optics — ICSO 2006, edited by Errico Armandillo, Josiane Costeraste, Nikos Karafolas, Proc. of SPIE Vol. 10567, 1056721 · © 2006 ESA and CNES
CCC code: 0277-786X/17/$18 · doi: 10.1117/12.2308080

A COMPARATIVE ANALYSIS AT ENGINEERING LEVEL OF DISPERSIVE AND FOURIER TRANSFORM SPECTROMETERS FOR MTG SOUNDING APPLICATIONS

Mathieu Quatrevalet[(1)], Donny Aminou[(2)], Jean-Loup Bézy[(3)]

[(1)] RHEA System S.A., New Tech Center, Avenue Einstein 2a, B-1348 Louvain-La-Neuve, Belgium
Consultant at the European Space Agency, ESTEC, Directorate of the Earth Observation Programmes, Earth Observation Projects Department
P.O. Box 299, 2200 AG Noordwijk, The Netherlands
e-mail: mathieu.quatrevalet@esa.int

[(2)] [(3)] European Space Agency, ESTEC, Directorate of the Earth Observation Programmes, Earth Observation Projects Department
P.O. Box 299, 2200 AG Noordwijk, The Netherlands
e-mails: donny.aminou@esa.int jean-loup.bezy@esa.int

ABSTRACT

Sounding measurements with high spatial resolution (better than 10 km horizontal and 1 km vertical) and repeat cycles better than an hour over the full Earth disk will enhance the ability of National Meteorological Services to initialise models of observations of temperature, moisture and winds.
To meet those needs, trade-off's were performed during the Meteosat Third Generation (MTG) mission study (2003-2005) where preliminary instrument concepts for the Infra-Red Sounding (IRS) mission were investigated allowing at the same time to consolidate the technical requirements for the overall system study. The trade-off's demonstrated that two types of instrument could fulfill the requirements: a Fourier Transform Spectrometer and a Dispersive Spectrometer.
This paper aims at comparing these two MTG-IRS sensor concepts by highlighting the differences in the constraints imposed on the characteristics and required performance at hardware level. In addition, technology criticalities and some other aspects are discussed qualitatively.

1. INTRODUCTION

The primary objective of the Infra-Red Sounding (IRS) mission of the Meteosat Third Generation (MTG) programme is "to enhance the National Meteorological Services' (NMS) ability to initialize Numerical Weather Prediction (NWP) models with more realistic information on temperature and moisture" thanks to "infrared soundings with high spatial [better than 10 km and 1 km vertical] and spectral [up to 0.5 cm^{-1}] resolution, and temporal sampling of a fraction of an hour" over the full Earth disk [1]. Such a short repeat cycle and large spatial coverage is made possible by the geostationary observing technique.

Proc. '6th Internat. Conf. on Space Optics', ESTEC, Noordwijk, The Netherlands, 27-30 June 2006 (ESA SP-621, June 2006)

Although referred to as a *sounder* with regard to its user requirements, the MTG-IRS sensor would rather be described, with regard to its technical requirements, as an *imaging spectrometer*. The purpose of imaging spectrometry is indeed "to measure the energy or quanta collected from an object as a function of two spatial dimensions and one spectral dimension" [3] forming a discrete data cube.

At instrument level, this is accomplished thanks to one or several two-dimensional detector arrays, hereafter referred to as Focal Plane Arrays (FPA) which "collect signal [...] as a function of column number, row number, and exposure number" [3]. The data gathered from each exposure corresponds to a slice of a "raw data cube" whose dimensions do not necessarily correspond directly to the two spatial and one spectral dimensions of the hyperspectral data cube. For each dimension of the raw data cube, the acquisition can take place simultaneously for all the cells along this dimension or one after the other. Different types of instrument principles and architectures are associated with some of these various ways of successively scanning through all the cells of the raw data cube within an allocated amount of time. In the particular case of MTG-IRS, two instrument concepts have been selected in the course of the MTG mission study and are currently being evaluated: a Fourier Transform Spectrometer (FTS) and a Dispersive Spectrometer (DS). The associated instrument principles are recalled in part 2.

For the same final data cube, it can be shown that the practical implementation of each instrument principle places different constraints on the characteristics and required performances at hardware and/or software level. It is the intent of the present document to qualitatively highlight these differences in the particular case of the DS and FTS concepts and in the frame of the MTG-IRS technical requirements. This

shall be done in two distinct steps: first by sizing some instrument parameters directly from the spectral, spatial and temporal performance requirements which can be fulfilled by design (part 3), and second by examining how the necessity to minimize non-scene-photonic noise sources for reaching the best radiometric performance can be translated into different design constraints at hardware level (part 4).

2. INSTRUMENT PRINCIPLES

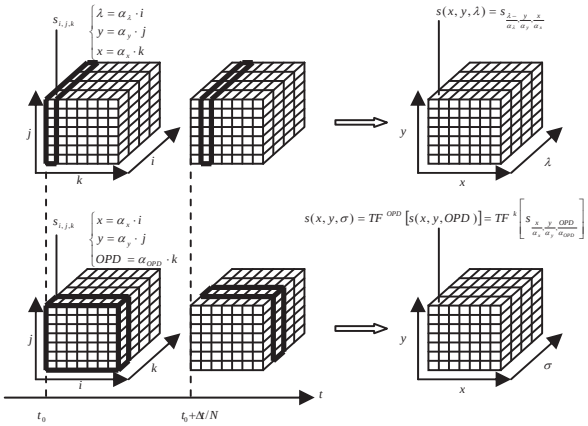

Figure 1 – Instrument principle and correspondence between the raw data cube and the final data cube for a Dispersive Spectrometer (top) and for a Fourier Transform spectrometer (bottom)

Fig. 1 shows the "instantaneous domain of view" of each concept inside the raw data cube with thick edges, and the correspondence between the coordinate system of the raw data cube and that of the hyperspectral data cube. In order to emphasize the different "orientation" of the two-dimensional arrays, all the cubes on Fig.1 are positioned so that the spatial plane is in the plane of the figure.

For the DS concept, each two-dimensional array is aligned with one spatial dimension – referred to as y on figure 1 - and with the spectral dimension of the hyperspectral data cube. Therefore the array row index j is proportional to the spatial dimension y and the array column index i is proportional to λ. For the FTS concept, the array is fully aligned with the spatial plane: i is proportional to x and j is proportional to y.

In order to reconstruct the third dimension, N frames are read out at a constant Temporal Sampling Interval (TSI) during the available acquisition time Δt while a certain instrument state parameter is scanned proportionaly to time: the instrument Line-Of-Sight (LOS) along x for the DS, and the Optical Path Difference (OPD) for the FTS. As a result, the exposure number k is proportional to x for the DS while it is proportional to the OPD for the FTS. A Fourier Transform along the OPD / exposure number axis gives access to the spectrum.

Assuming that the signal recorded at each frame by each detector of each array corresponds to a cell of the raw data cube (i.e., no spatial, spectral or temporal binning or filtering is considered), and that all the time available per exposure is used for integration, the signal in electrons is approximately equal to:

$$S^{DS} = A\Omega^{DS} \cdot \tau^{DS} \cdot \eta \cdot \overline{L} \cdot \delta\sigma_0 \cdot \frac{\Delta t}{N^{DS}} \qquad (1)$$

for the DS and

$$S^{FTS} = \Gamma \cdot A\Omega^{FTS} \cdot \tau^{FTS} \cdot \eta \cdot \overline{L} \cdot \Delta\sigma \cdot \frac{\Delta t}{N^{FTS}} \qquad (2)$$

for the FTS,

where $A\Omega$ is the geometrical throughput associated with a single detector, τ is the transmittance of the optical train associated with the array, η is the detector quantum efficiency, $\delta\sigma_0$ is the width of a spectral channel, $\Delta\sigma$ is the spectral range of the light incident on the array, $\overline{L}$ is the mean value over this range of the target spectral radiance in photonic units, and Γ is equal to 1 for a frame at Zero Path Difference (ZPD) and ½ for a frame away from ZPD.

3. INSTRUMENT SIZING

As for any spectrometry mission, the major purpose of the MTG-IRS requirements [1] is to size the hyperspectral data cube. From a purely mathematical perspective, there is a need for 9 parameters to fully specify the cube: the coverage, sampling interval and resolution along each dimension. However, a certain number of additional assumptions apply for MTG-IRS:

- same Spatial Sampling Distance (SSD) and resolution along both spatial dimensions *x* and *y*,
- same spatial coverage along both spatial dimensions, equal to the projected size of the Earth on its tangential plane at Nadir.

In addition to the remaining 6 spectral-spatial parameters, the only other specifications that are needed for a preliminary sizing of the instrument are the repeat cycle which corresponds to the sampling interval along the temporal dimension, and the dynamic range which corresponds to the coverage along the radiometric dimension.

3.1 Spatial sizing and scanning principle

Band	IRS-1 to IRS-4	IRS-5 to IRS-7
SSD $\underset{\leftrightarrow}{\delta X}$ (km)	6	3
Coverage ΔX (km)	11150	
Repeat cycle Δt (mn)	30	

Table 1 – Specified SSD, spatial coverage and repeat cycle for MTG-IRS (see table 2 for the definition of the spectral bands, IRS-1 to IRS-7)

Table 1 presents the key spatial and temporal requirements. The SSD is achieved by choosing the right detector pitch / focal length combination for the FTS along both spatial dimensions and along the field direction for the DS, and the right scan speed / TSI combination for the DS along the scan direction.

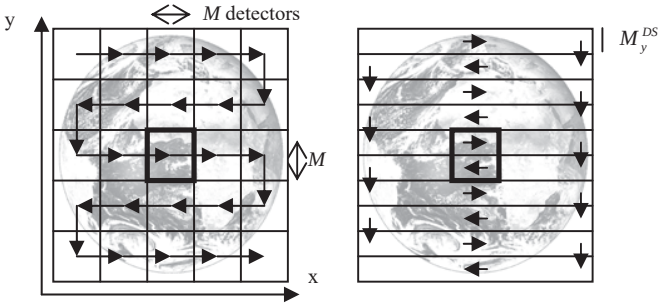

Figure 2 – Scanning principle for the FTS concept (left) and for the DS concept (right). The square with thick edges represents the restricted spatial domain for simplification of the study.

While Fig. 1 implicitly assumed that the full image can be covered with a single scan (of the *x* axis or of the OPD), this would require array sizes of up to 3700x3700 detectors (FTS concept, IRS-5 to IRS-7). In reality, a high number of square sub-images for the FTS and strips along the scan direction for the DS are acquired successively to cover the Earth by sequentially moving the LOS, as shown on Fig. 2. The number of required steps or scans is driven by the instrument field of view, which is limited by a theoretical limit (described for instance by Beer [2]) on the array dimension in detectors due to self-apodization (FTS only), the limits of optical design with regard to aberrations and vignetting, and the limits of IR FPA technology in terms of number of detectors and array physical size.

Yet it is clear from Fig. 2 that, neglecting the time lost for stepping from one LOS position to the other, the spatial extent of this analysis can be restricted to a spatial domain equal to one subimage of the FTS, by rewriting the requirements in the following way:

$$\begin{aligned} \Delta X &\leftarrow \underset{\leftrightarrow}{\delta X} \cdot M \\ \Delta t &\leftarrow \Delta t \cdot \left(\frac{\underset{\leftrightarrow}{\delta X} \cdot M}{\Delta X} \right)^2 \end{aligned} \tag{3}$$

where M is the size in detectors of the FTS array (assumed square). The number of frames that are necessary for the DS to acquire this subimage is:

$$N^{DS} = r \cdot M \,, \tag{4}$$

where r is the ratio between the array size of the FTS and the array size of the DS along the cross-scan direction:

$$r = \frac{M}{M_y^{DS}} \tag{5}$$

with M_y^{DS} the DS array size in detectors along the field direction. As for the number of frames for the FTS, N^{FTS}, and the size of the array along the spectral direction for the DS, M_x^{DS}, they are linked to the spectral requirements which are discussed in next paragraph.

3.2 Spectral sizing

As already stated in part 2, a DS provides an approximately constant Instrument Spectral Response Function (ISRF) and uniform spectral sampling on the wavelength scale while a FTS provides a constant ISRF and a uniform spectral sampling on the wavenumber scale. In order to have a unique specification applicable for both concepts, the spectral resolution is specified in [1] in terms of the required resolving power $\Re$ at the central wavelength (DS) or wavenumber (FTS) of the band; these specifications are recalled in table 2.

Band	IRS-1	IRS-2	IRS-3	IRS-4	IRS-5	IRS-6	IRS-7
$\sigma_{\min}$ (cm^{-1})	700	770	980	1070	1210	1600	2000
$\sigma_{\max}$ (cm^{-1})	770	980	1070	1210	1600	2000	2250
$\Re$	1470	1400	2070	1344	2248	2880	3400
$\delta\sigma_0$ (cm^{-1})	0.50	0.63	0.50	0.85	0.63	0.63	0.63

Table 2 – MTG-IRS spectral requirements

It can be shown that this is equivalent to specifying an equal number of spectral resolution elements for both concepts; in addition for the DS, a requirement in [1] explicitly specifies a spectral oversampling factor of 2. The resulting number of spectral samples for the DS, which is also the required array size in detectors along the spectral direction M_x^{DS}, is shown in table 3.

For the FTS, the spectral oversampling requirement is implicit: the spectral resolution $\delta\sigma_0$ is defined as the FWHM of the unapodized spectral response function, and it is a well known result (cf Beer [2], for instance) that the ratio between this quantity and the spectral sampling for an ideal FTS is 1.207. This required spectral sampling gives access to the maximum OPD of the interferometer; by considering the minimum sampling wavenumber, which is imposed by the Shannon sampling theorem (twice the maximum frequency of the measured spectrum, $\sigma_{\max}$), the minimum number of interferogram samples which is also the number of frames for the FTS can be calculated. The results are also shown in table 3.

Band	IRS-1	IRS-2	IRS-3	IRS-4	IRS-5	IRS-6	IRS-7
M_x^{DS} (SC7)	280	672	364	330	1248	1280	800
N^{FTS} (SC7)	1859	1877	2583	1719	3066	3832	4310
N^{FTS} / M_x^{DS} (SC7)	**6.6**	**2.8**	**7.1**	**5.2**	**2.4**	**3.0**	**5.4**
M_x^{DS} (SC2)	1646				3328		
N^{FTS} (SC2)	2921				4310		
N^{FTS} / M_x^{DS} (SC2)	**1.8**				**1.3**		

Table 3 – Required array size along the spectral direction for the DS and number of frames for the FTS

Two study cases are distinguished in table 3: in the first case ("SC7", for "Study Case 7 FPAs"), each IRS band enjoys a dedicated FPA, in the second case ("SC2", for "Study Case 2 FPAs") the bands are grouped according to their spatial resolution and thus covered by only two distinct FPAs.
On one hand, with SC7, the detector characteristics (material, cutoff wavelength) can be fine-tuned independently for each band, which is highly desirable from a performance point of view.
On the other hand, SC2 is by far preferable from a cost point of view, because each additional FPA and its associated optical train, coolers and electronics lead to a significant increase of volume and mass. But for the FTS, inherently to the instrument principle, it is detrimental to the performance since each detector records the signals corresponding to all wavenumbers covered by the FPA simultaneously and cannot be optimized for all the bands covered; while, for the DS the "stichting" technique makes it possible to implement several distinct detector modules along the spectral direction with different characteristics on the same monolithic ROIC, at the price of the presence of dead zones of a few spectral channels between detector modules.

In fact, as far as the DS concept is concerned, for array sizes so large as the ones predicted in table 3 for SC2, stitching is bound to be necessary anyway due to the technological limits with regard to the maximum size of a single detector module. Even for SC7, the DS array size along the spectral direction reaches values over 1000 detectors in the MWIR range, and this is *imposed* by the requirements, while the FTS array size M can be *chosen* as small as possible by the designer.

The pixel readout frequencies per array can be calculated for each concept thanks to:

$$f_{ro}^{DS/FTS} = \frac{N^{DS/FTS}}{\Delta t} \cdot M_x^{DS/FTS} \cdot M_y^{DS/FTS} \quad (6)$$

which leads, by injecting Eqs. (4) and (5) for the DS, to

$$f_{ro}^{DS} = \frac{M_x^{DS}}{\Delta t} \cdot M^2 \;/\; f_{ro}^{FTS} = \frac{N^{FTS}}{\Delta t} \cdot M^2 \quad (7)$$

The ratio between the pixel readout frequencies per arrray for the FTS concept and for the DS concept appears to be independent from r: it is simply N^{FTS} / M_x^{DS}. It is indicated in table 3 for each study case: the FTS is disadvantaged, by factors up to 7 (IRS-3, SC7). However this corresponds to the readout frequency at the output of each array, thus at the level of the raw interferogram; what can be concluded from these numbers is that the internal readout rates are higher for the FTS and that more on-board processing is needed than for the DS in order to bring the downlink data rate at the same levels.

3.3 Radiometric sizing

The primary purpose of the radiometric sizing of the detection chain is to size the integration capacitance of individual readout cells so that it matches the maximum expected signal. Assuming that only the surface underneath the detector is available for implementation of the capacitance, there is a technological limit to its value. With p_{det} the detector pitch, c_0 the feasible surface capacitance density and $V_{\max}$ the ROIC output voltage swing, the maximum input-referred full well capacity per detector in electrons is:

$$S_0 = c_0 \cdot \frac{V_{\max}}{q} \cdot p_{\text{det}}^2 \quad (8)$$

where q is the charge on the electron. If the maximum signal exceeds this value, temporal oversampling is necessary to avoid saturation, with the temporal oversampling factor given by

$$k_{over} = INT\left(\frac{S_{\max}}{S_0}\right) + 1 \quad (9)$$

where $S_{\max}$ is the maximum signal, which can be computed thanks to Eq. (1) and (2) using the specified maximum target spectral radiance for $\overline{L}$.

Another technological limitation not yet taken into account is the maximum pixel readout frequency per video output, $f_{\max}$. This limitation is overcome by increasing the number of video outputs N_{out} of the ROIC:

$$N_{out} = INT\left(\frac{k_{over} \cdot f_{ro}}{f_{\max}}\right) + 1 \quad (10)$$

where f_{ro} can be calculated from Eq. (7).

Using (8), (9) and (10), a numerical example for the required temporal oversampling and number of video outputs is presented in table 4 for both the DS and the FTS, and for the two afore-mentioned study cases, with realistic values for c_0, $V_{\max}$, τ^{DS}, τ^{FTS} and for an entrance aperture of 0.3 m (value currently considered in the baseline concepts), a detector pitch of 50 microns (IRS-5 to IRS-7) / 100 microns (IRS-1 to IRS-4), and for *M* = 256 (IRS-5 to -7) / 128 (IRS-1 to -4).

Band	IRS-1	IRS-2	IRS-3	IRS-4	IRS-5	IRS-6	IRS-7
k_{over} (DS) (SC7)	1	1	1	1	1	1	1
k_{over} (FTS) (SC7)	2	4	1	2	1	1	1
N_{out} (DS) (SC7)	1	1	1	1	2	3	2
N_{out} (FTS) (SC7)	13	25	9	12	11	13	15
k_{over} (FTS) (SC2)	5				1		
N_{out} (FTS) (SC2)	49				15		

Table 4 – Temporal oversampling factor and number of video outputs for a particular set of parameters

Because the level of the signals recorded by the FTS are orders of magnitude higher than the signals recorded by the DS, temporal oversampling is needed for the FTS in the LWIR range while it is not for the DS. This further increases the readout rate at the output of each array, already found to be higher than for the DS in paragraph 3.2. These high pixel readout frequencies impose a great number of video outputs. This number increases and becomes even unrealistic when considering SC2, because a broader spectral range is then incident on the detectors (the results for the DS are unchanged with respect to SC7 and not shown in table 4, because the incident signal is the same).

4. DESIGN CONSTRAINTS RELATED TO RADIOMETRIC RESOLUTION

While the spatial, spectral, temporal requirements and the dynamic range are inputs to the sizing process and can be directly translated into physical or operational characteristics of the hardware (array sizes, readout rates, integration capacitance), the radiometric resolution may be considered as the "error function" of the sizing process, in the sense that it is only by "playing" with the remaining degrees of freedom and with the performances of the available detector technologies that the designer can optimize it. Since it is not the intent of this document to perform such a complete trade-off, a very simple approach has been used.
The fundamental limit of radiometric performance is related to the photonic noise associated with the photosignal generated by the photons from the target scene, and whose variance is equal to the recorded signal itself. In a very simplified analysis, this Scene-Photonic-Noise-Limited (SPNL) regime can be arbitrarily considered as a goal, regardless of the specified radiometric resolution (which may or may not require SPNL operation). Defining the maximum tolerable variance of any other noise contribution as the variance of the typical scene photonic noise enables to highlight several trends in terms of the different design constraints placed on hardware by each concept.

4.1 Considered noise sources

Three additional noise sources have been considered: the photonic noise due to the photosignal generated by the thermal emission from the instrument, the shot noise due to the dark current signal, and the readout noise due to the ROIC. Similarly to the photonic noises, the variance of the dark current shot noise is equal to the dark signal itself:

$$\sigma^2_{dark} = I_d \cdot \frac{\Delta t}{N} \quad (11)$$

where I_d is the dark current in e-/s.

The variance of the readout noise must account for temporal oversampling, i.e. the noise of each readout adds quadratically to the total noise for a cell of the raw data cube:

$$\sigma^2_{ro} = k_{over} \cdot \left(\frac{v_{ro}}{CF}\right)^2 \quad (12)$$

where v_{ro} is the total RMS noise voltage generated at each readout by all contributors in the readout

electronics up to the input of the A/D converter (which is supposed not to add any further noise thanks to a sufficient number of bits) and CF is the conversion factor, which is by definition equal to the output voltage swing divided by the integration capacitance:

$$CF = V_{\max} \cdot \left(\frac{S_{\max}}{k_{over}} \right)^{-1} \quad (13)$$

4.2 Dark current and FPA cooling

Equations (1) or (2) (away from ZPD for the FTS) and (11) yield the maximum tolerable dark current for each concept:

$$I_{d\ \max}^{DS} = A\Omega \cdot \tau^{DS} \cdot \eta \cdot \overline{L} \cdot \delta\sigma_0 \quad (14)$$

$$I_{d\ \max}^{FTS} = \frac{1}{2} \cdot A\Omega \cdot \tau^{FTS} \cdot \eta \cdot \overline{L} \cdot \Delta\sigma \quad (15)$$

which shows that, for the same detector size, the FTS concept is inhenrently much more immune to dark current, by a factor $\frac{1}{2} \cdot \frac{\tau^{FTS}}{\tau^{DS}} \cdot \frac{\Delta\sigma}{\delta\sigma_0} >> 1$.

Thanks to recent dark current models, Eq. (1) and (2) have been translated into requirements on the maximum FPA temperature; the details are not presented here but the results are shown in table 5 for SC7.

Band	IRS-1	IRS-2	IRS-3	IRS-4	IRS-5	IRS-6	IRS-7
$T_{FPA\max}^{DS}$ (K)	44	49	60	68	71	87	106
$T_{FPA\ \max}^{FTS}$ (K)	53	63	74	82	91	110	129

Table 5 – Maximum FPA temperature for each concept with SC7 and realistic dark current models

The DS concept is clearly more demanding in terms of FPA cooling temperature, because of the weaker photosignal from the target scene; this disadvantage has already been noted in literature [4].

4.3 Instrument background and cooling of the optics

Without a detailed optical design, it is difficult to assess the background flux incident on the FPA. However, a significant difference exists between the FTS and the DS: while the radiation from all the optical elements are spectrally filtered in the same way as the radiation from the scene for the FTS (by the bandpass filter associated with the considered FPA), two types of contributions must be distinguished for the DS concept:

- the contributions along the nominal optical path from the elements upstream of the slit assembly, which are spectrally filtered by the ISRF of the instrument and therefore spectrally integrated over the width of a spectral channel like the radiation from the scene,
- the contributions out of the nominal optical path from the elements downstream of the slit plane, including the slit assembly itself, which are only filtered by the bandpass filter in front of each detector module and therefore spectrally integrated over $\Delta\sigma$.

The contribution from these elements to the background signal can be roughly modelled by a gray body with effective emittance ε, seen with the same geometrical throughput as the scene. Using Eqs. (1) and (2), the temperature $T_{\max}$ for which the contribution of the instrument background to the photosignal is equal to the contribution of the target scene verifies:

$$\varepsilon \cdot \overline{BB}(T_{\max}) = \overline{L} \cdot \tau^{DS} \cdot \frac{\delta\sigma_0}{\Delta\sigma} \quad (16)$$

for the DS and

$$\varepsilon \cdot \overline{BB}(T_{\max}) = \frac{1}{2} \cdot \overline{L} \cdot \tau^{FTS} \quad (17)$$

for the FTS, which shows that the DS is more sensitive to the instrument background, by the same factor as for the dark current, in paragraph 4.2. Using Eqs. (16) and (17), the maximum temperature of the optics has been computed for a realistic value of ε. The numerical results are shown in table 6 for SC7.

Band	IRS-1	IRS-2	IRS-3	IRS-4	IRS-5	IRS-6	IRS-7
$T_{\max}^{DS}$ (K)	104	106	124	133	132	151	170
$T_{\max}^{FTS}$ (K)	203	212	223	229	238	249	257

Table 6 – Maximum tolerable temperature of the optics for each concept and for a realistic emittance

Just as for the FPA cooling, the DS is more demanding for the cooling of the optics than the FTS. A technological solution to this, which has already been used successfully with dispersive spectrometers in the thermal infrared [5], is the use of a Linear Variable Filter (LVF) for suppression of the radiation from the proximity optics. The trade-off for the DS is then between an added development effort (LVF) or more cooling needs.

4.4 Readout noise and ROIC dynamic range

While the temporal oversampling factor and conversion factor involved in Eq. (12) are imposed by the sizing of the detection chain, v_{ro} is a technological parameter and the requirement on the maximum tolerable value of readout noise can be considered as a requirement on the minimum value of the ROIC dynamic range $DR_{\min}$, classically defined as the ratio between $V_{\max}$ and v_{ro}. Combining Eqs. (12), (13) and (9), $DR_{\min}$ verifies:

$$S_{typ} = \left(DR_{\min}\right)^{-2} \cdot \frac{S_{\max}^2}{INT\left(\frac{S_{\max}}{S_0}\right)+1} \qquad (18)$$

where S_{typ} is the typical signal due to the target scene and computed from Eq. (1) and (2).
Two distinct behaviours of Eq. (18) can be distinguished: if $S_{\max} < S_0$ (no temporal oversampling) then $DR_{\min}$ is proportional to the square root of the maximum signal:

$$DR_{\min} = \sqrt{\beta \cdot S_{\max}}, \qquad (19)$$

If $S_{\max} >> S_0$ (high temporal oversampling) then $DR_{\min}$ converges towards a constant value:

$$DR_{\min} = \sqrt{\beta \cdot S_0} \qquad (20)$$

In Eqs. (19) and (20), β is defined by:

$$\beta = \frac{\overline{L}_{\max}}{\overline{L}_{typ}} \qquad (21)$$

β is a concept-independent measure of the specified "dynamic range" in terms of target spectral radiances; its numerical values are indicated in table 7.

Band	IRS-1	IRS-2	IRS-3	IRS-4	IRS-5	IRS-6	IRS-7
β	1.4	1.9	2.4	2.3	1.6	1.4	4.0

Table 7 – Ratio between the specified maximum and typical target radiances per IRS band

With the same parameters as for the numerical example of paragraph 3.3, $DR_{\min}$ has been quantified for SC7 and the results are shown in table 8.

Band	IRS-1	IRS-2	IRS-3	IRS-4	IRS-5	IRS-6	IRS-7
$DR_{\min}$ (DS) (dB)	75	78	76	78	61	52	57
$DR_{\min}$ (FTS) (dB)	88	89	90	90	87	78	81

Table 8 – Minimum ROIC dynamic range for each concept and for SC7

The FTS is strikingly more demanding in terms of FPA dynamic range, with values up to 90 dB which is considered as very challenging with the current technologies and may call for the use of advanced on-chip techniques such as skimming or non-linear conversion.

5. TECHNOLOGY CRITICALITIES

It must be emphasized that the discussions on dark current issues in the LWIR range are based on extrapolations of detector performances working with cutoff wavelengths under 12.5 microns. The 12.5-15 micron region has not yet been proved by European manufacturers for large 2D arrays, consequently there is a development risk associated with this LWIR range.

Although this development risk will be the same for both concepts at first order (realization of arrays with a sufficiently high yield and uniformity for these cutoff wavelenghts), parts 3 and 4 showed that, in a second phase, the emphasis will have to be put on different aspects of array developement for each concept:

- Manufacturing physically large arrays based on several detector modules by stitching/butting for the DS concept, and minimizing the dark current,
- Reaching high dynamic ranges for the ROIC of the FTS concept, and/or implementing on-chip advanced techniques such as skimming or non-linear conversion.

It is however difficult at this stage to determine which aspect presents the highest development risk.

6. OTHER ASPECTS

6.1 AOCS

Fourier transform spectrometers are known to be very susceptible to temporal fluctuations of the target spectrum. In the case of an imaging spectrometer, these fluctuations can be produced by the combination of a heterogeneity in the pixel (presence of a cloud) and any LOS instability or "jitter". Bennett has shown that even low jitter amplitudes can cause a rather high level of noise in the measured spectrum [6].

This is particularly critical in the configuration of MTG-IRS combining GEO orbit and relatively high

spatial resolutions (6 km / 3 km), because the same angular LOS instability will lead to much higher fluctuations of the signal than in LEO orbit (by a factor around 40). This requirement on LOS stability applies over the full dwell time Δt of the FTS concept, i.e. 8 s for the numerical example used throughout this document.

For the DS concept, not only are the requirements on LOS stability much less stringent in terms of amplitude (they are in this case linked to spatial requirements), but they apply only over the integration time per spatial sample, i.e. a few milliseconds. This is quantified in table 9 for the numerical example used throughout this document; the dwell time is presented for each concept, along with the corresponding maximum admissible angular drift, based on the relevant requirement [1] for a maximum LOS instability of 11 µrad.

Concept	Dwell time (ms)	Maximum drift (µrad/s)
DS	7.8	1410
FTS	8000	1.4

Table 9 – Dwell time and associated maximum drift for each concept

As a consequence, it is foreseen that the requirements on AOCS at spacecraft level will be much more severe for the FTS concept than for the DS concept. Given the sensitivity of the FTS concept not only to the amplitude but also to the frequency spectrum of jitter, greater care will have to be put in the mechanical design of the optical bench and spacecraft (micro-vibrations) and/or the interferogram processing.

6.2 Spectral calibration

While the radiometric calibration process is likely to be similar, the spectral calibration process will be different for each concept. Regardless of the estimated performance of the spectral calibration algorithm in terms of radiometric accuracy, it can be anticipated that:

- A simpler, deterministic instrument model is expected to be usable for the FTS,
- The spectral stability of the FTS concept is bound to be higher than the DS concept. Indeed, it is felt that the great sensitivity of the DS concept to array mis-alignements or distortions along the spectral direction will make it challenging to reach the required spectral stability (currently specified at 10^{-6}), whereas the FTS is inherently stable thanks to the use of a stabilized laser source for interferogram sampling.

7. CONCLUSION

With the help of a simplified instrument model, the differences between a DS concept and FTS concept have been highlighted in terms of the constraints directly or indirectly placed at hardware level by the challenging MTG-IRS technical requirements. While the DS concept requires physically larger and architecturally more complex (non-monolithic) arrays, and a more agressive cooling of both the FPA and the optics, the FTS concept calls for the use of more advanced ROICs with more video outputs and a higher dynamic range, and also requires more on-board processing due to the high internal data rates.

As far as other aspects are concerned, each concept has its own specific weaknesses and strengths. The FTS concept puts higher requirements on the AOCS, and further requirements on processing for detection and removal of potential spectral ghosts due to jitter. The spectral calibration is bound to be more critical for the DS concept.

All things considered, no key argument makes it possible to make a clear statement on the preference for one concept or the other from an engineering point of view at this stage of the study. Both concepts must be analyzed in more depth and it is only at a more advanced stage, possibly at breadboard level, that such arguments may appear. Alternatively, the decision may be motivated by considerations on the end users' side.

REFERENCES

1. EUMETSAT, *MTG Mission Requirements Document*, Doc. No. EUM/MTG/SPE/02/0015, Issue 1.2, 12 October 2004 (Accessible on the EUMETSAT website, www.eumetsat.int).
2. Reinhard Beer, *Remote Sensing by Fourier Transform Spectrometry*, *Chemical Analysis vol. 120*, Wiley Interscience, 1992.
3. R Glenn Sellar and Glenn D. Boreman, *Comparison of relative signal-to-noise ratios of different classes of imaging spectrometers*, Applied Optics Vol. 44, No. 9, pp. 1614-1624, 2005.
4. Michael E. MacDonald et al, *Architectural Trades for an Advanced Geostationary Atmospheric Sounding Instrument*, Proceedings from ASP Conference Series, Vol. 4, 2001.
5. Nahum Gat et al, *Thermal Infrared Imaging Spectrometer (TIRIS) Status Report, Infrared Technology and Applications XXIII*, Proceedings of SPIE Vol. 3061, pp. 284-29, 1997.
6. Charles L. Bennett, *The effect of jitter on an imaging FTIR spectrometer, Infrared Imaging Systems: Design, Analysis, Modeling and Testing VIII*, Proceedings of SPIE Vol. 3063, pp. 174-184, 1997.